

An Investigation on  $\gamma$  induced activation reactions on human essential elements\*

LÜ Cui-Juan (吕翠娟),<sup>1</sup> MA Chun-Wang (马春旺),<sup>1,†</sup> LIU Yi-Pu (刘一璞),<sup>2</sup>  
ZHANG Wen-Gang (张文岗),<sup>2</sup> and ZUO Jia-Xu (左嘉旭)<sup>3,‡</sup>

<sup>1</sup>Institute of Particle and Nuclear Physics, Henan Normal University, Xinxiang 453007, China

<sup>2</sup>College of Physics and Electronic Engineering, Henan Normal University, Xinxiang 453007, China

<sup>3</sup>Department of Nuclear and Radiation Safety Research,

Nuclear and Radiation Safety Center (MEP), Beijing 100082, China

(Received February 26, 2015; accepted in revised form May 10, 2015; published online June 20, 2015)

In radiotherapy, the energy of the  $\gamma$  rays used could be larger than 10 MeV, which would potentially activate stable nucleus into a radioactive one. The  $\gamma$  induced reactions on some of the human essential elements are studied to show the probability of changes of nuclei. The Talys 1.4 toolkit was adopted as the theoretical model for calculation. The reactions investigated include the  $(\gamma, n)$  and  $(\gamma, p)$  channels for the stable Na, Mg, Cl, K, Ca, and Fe isotopes, with the incident energy of  $\gamma$  ranging from 1 to 30 MeV. It was found that the cross sections for the reactions are very low, and the maximum cross section is no larger than 100 mb. By considering the threshold energy of the channel, the half-life time of the residue nucleus, and the percentage of the element accounting for the weight and its importance in the body, it is suggested to track the radioactive nuclei  $^{22}\text{Na}$ ,  $^{41}\text{Ca}$ , and  $^{42,43}\text{K}$  after  $\gamma$  therapy. The results might be useful for medical diagnosis and disease treatment.

Keywords: Photon activation,  $\gamma$  therapy, Human essential element, Optical model, Talys

DOI: [10.13538/j.1001-8042/nst.26.030503](https://doi.org/10.13538/j.1001-8042/nst.26.030503)

## I. INTRODUCTION

Nuclear technology has found many applications in medical diagnosis and disease treatment, such as the X/ $\gamma$ -CT, X/ $\gamma$ -cure, and positron emission computed tomography (PET), etc. In radiation therapy, most of the side effects are predictable and expected, thus are avoidable in the patient's normal tissue. It is desirable to understand the origination of side effects and ways to reduce the unwanted side effects. Besides the complex biochemical effects [1–3] of  $\gamma$  rays on molecules, mainly through ionization and Compton scattering [4],  $\gamma$  rays can induce a nuclear reaction through positron-electron pair production and photon activation reactions. Though the possibility is quite low, the high energy  $\gamma$  rays ( $E_\gamma > \sim 10$  MeV) can also induce nuclear activation reactions and activate the stable nucleus into radioactive nucleus. It is well known that around  $\gamma = 15$  MeV, the nucleus has a strong  $\gamma$ -absorption ( $\gamma$ -emission) rate because of the giant dipole resonance [5–8], in which stable nuclei can be activated to unstable ones via  $(\gamma, n)$  or  $(\gamma, p)$  reactions. In particular, for nuclei with small mass numbers, the  $(\gamma, n)$  cross section may form a peak below 15 MeV, for example,  $^{13}\text{C}$  [8],  $^{17}\text{O}$  [9],  $^{18}\text{O}$  [10] and  $^{29}\text{Si}$  [11]. The energy of  $\gamma$  rays used in  $\gamma$  cure can be larger than 10 MeV, which potentially can induce  $\gamma$ -activation reactions. The residue nucleus of  $\gamma$ -activation reactions in potential can be one kind of inner radioactivity and harmful to normal tissue if it has a long half-life. It is interesting to study the  $\gamma$ -induced reactions on the elements forming the human body in the energy range of  $\gamma$ -cure. Motivated by this reason, in this article, the  $\gamma$ -induced

reactions on the isotopes of essential elements of the human body will be investigated. Meanwhile, the possible nuclear activation reactions for these isotopes will be discussed.

## II. METHODS

The  $\gamma$  induced reactions on the nucleus are called photon-nucleus reactions, which have attracted much attention in nuclear physics. A lot of  $\gamma$  induced reactions on various isotopes have been measured for different purposes. The optical model is very successful in predicting the  $\gamma$  induced reactions for outgoing particles. In the Talys toolkit [12], the ECIS-06 code has been implanted as a subroutine to deal with the optical model calculations [13, 14]. The Talys toolkit is usually used in the analysis of experiments and generating of nuclear data. With different adjustable parameters, the Talys toolkit can reproduce the neutron induced reactions on the nuclei with a mass of  $A > 30$ . While for a nucleus of  $A < 30$ , the parameters in Talys should be adjusted to coincide with the experimental results [14, 15]. Talys version 1.4 is adopted in this work. We will not describe the model since the aim of this work is not to introduce the physics of the Talys. The complete description of Talys1.4 can be found in the user manual [12]. The long half-life time radioactive nuclei produced from stable nuclei by  $\gamma$ -activation reactions will be the focus. The  $(\gamma, n)$  and  $(\gamma, p)$  channels will be calculated by considering whether the residue nucleus is unstable and has a long half-life time. The calculated results are also compared to the experimental results extracted from the EXFOR library [16]. The default parameters in Talys1.4 are adopted, since we do not aim to exactly reproduce the measured data, which requires the careful adjustment of parameters. All the natural abundance data and the half-life time of the isotopes are taken from the National Nuclear Data Cen-

\* Supported by the Plan for Scientific Innovation Talent of Henan Province (PSITHP) and the Young Teacher Project at Henan Normal University

† [machunwang@126.com](mailto:machunwang@126.com)

‡ [zuojiaxu@chinansc.cn](mailto:zuojiaxu@chinansc.cn)

ter (NNDC) [17]. The knowledge about human elements in the following discussion is extracted from the website of the Micronutrient Information Center of Linus Pauling Institute (MICLPI) [18].

### III. RESULTS AND DISCUSSION

In medical experimentation, the samples of blood and hair are generally inspected. We study the  $\gamma$  induced reactions on the isotopes of Na, Cl, Ca, K, and Mg because they have a relatively large weight in the human body.

#### A. $^{23}\text{Na}(\gamma, n)^{22}\text{Na}$

Sodium has only one stable isotope,  $^{23}\text{Na}$ . For an adult, sodium accounts for 0.15% of the human body, most of which exists in bones (about 40–47%), extracellular fluids (about 44–50%), and blood (about 9–10%). The function of sodium is to maintain the balance of osmotic pressures and moisture inside and outside the cell and to assist in the normal operation of the nerves, heart, muscles, and other physiological functions [19]. The retention time of sodium is short in the body, and is discharged mainly by sweat and the renal system. The normal level of  $\text{Na}^+$  in blood is 136–146 mmol/L.

For the  $^{23}\text{Na}(\gamma, n)^{22}\text{Na}$  reaction, the residue  $^{22}\text{Na}$  is a radioactive nucleus, which decays to  $^{22}\text{Ne}$  via positron emissions with a half-life time of 2.60  $\text{y}$ .  $^{22}\text{Na}$  is used to create test-objects and point-sources for positron emission tomography. In nuclear accidents, the sodium isotopes are also indicators to estimate exposure to neutron radiation [15].

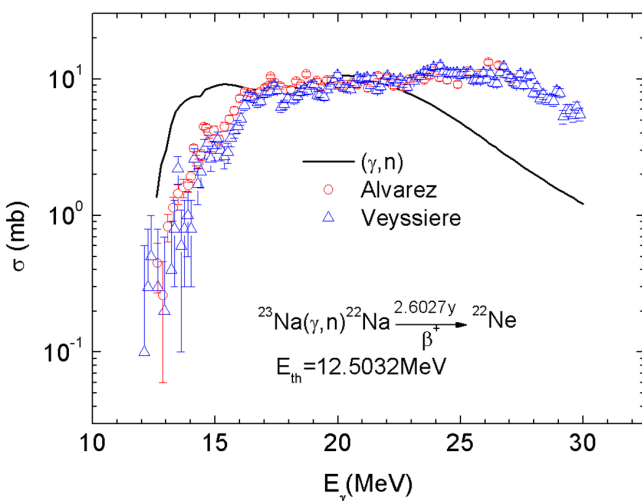


Fig. 1. (Color online) The results for the  $^{23}\text{Na}(\gamma, n)^{22}\text{Na}$  reaction. The calculated result is plotted as the solid line, and the measured ones are plotted as circles and triangles.

The cross section ( $\sigma$ ) of  $^{23}\text{Na}(\gamma, n)^{22}\text{Na}$  is plotted in Fig. 1. The calculated threshold energy ( $E_{\text{th}}$ ) for  $^{23}\text{Na}(\gamma, n)^{22}\text{Na}$  is 12.50 MeV, which agrees with the measured results. The

measured  $\sigma$  for the  $(\gamma, n)$  reaction by Alvarez *et al.* [20] and Veyssiére *et al.* [21] are consistent. When  $E_{\gamma} > E_{\text{th}}$ , the measured  $\sigma$  increases quickly with  $E_{\gamma}$ , but forms a plateau when  $E_{\gamma} > 16 \text{ MeV}$ . The calculated results overestimate the measured ones in  $12.5 \text{ MeV} < E_{\gamma} < 16 \text{ MeV}$ . The measured  $\sigma$  for  $^{23}\text{Na}(\gamma, n)^{22}\text{Na}$  within the range of  $16 \text{ MeV} < E_{\gamma} < 23 \text{ MeV}$  is around 10 mb. It could be necessary to track the  $^{22}\text{Na}$  in body after the  $\gamma$  cure since it has a long half-life and sodium accounts for a relatively large percentage of body weight.

#### B. $^{42}\text{Ca}(\gamma, n)^{41}\text{Ca}$ , $^{43}\text{Ca}(\gamma, p)^{42}\text{K}$ , and $^{44}\text{Ca}(\gamma, p)^{43}\text{K}$

Calcium is the most abundant mineral in the human body. About 99% of the calcium in the body is in bones and teeth, with the other 1% in the blood and soft tissues. Calcium is deposited in body and kept for a long time. The normal level of calcium in the blood is 1.55–2.10 mmol/L.

For the  $\gamma + \text{Ca}$  reaction, the three isotopes  $^{42}\text{Ca}$ ,  $^{43}\text{Ca}$ , and  $^{44}\text{Ca}$  (with the natural abundance 0.647%, 0.135%, and 2.08%, respectively), are considered. For the  $^{42}\text{Ca}(\gamma, n)^{41}\text{Ca}$ ,  $^{43}\text{Ca}(\gamma, p)^{42}\text{K}$  and  $^{44}\text{Ca}(\gamma, p)^{43}\text{K}$  channels,  $^{41}\text{Ca}$  decays into  $^{41}\text{K}$  via electron capture with a half-life of  $1.02 \times 10^5 \text{ a}$ ;  $^{42}\text{K}$  decays to  $^{42}\text{Ca}$  and  $^{43}\text{K}$  decays into  $^{43}\text{Ca}$ , both via electron emission with the half-lives of 12.32 h and 22.30 h, respectively. There are no natural  $^{42}\text{K}$  and  $^{43}\text{K}$  isotopes.

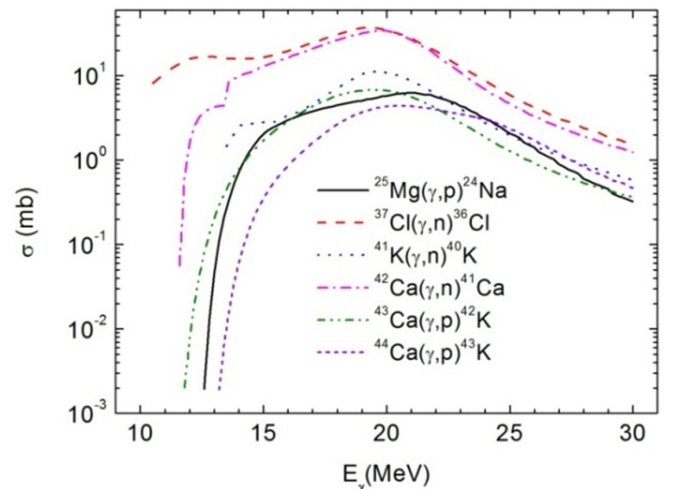


Fig. 2. (Color online) The calculated cross section for the  $^{25}\text{Mg}(\gamma, p)^{24}\text{Na}$ ,  $^{37}\text{Cl}(\gamma, n)^{36}\text{Cl}$ ,  $^{42}\text{Ca}(\gamma, n)^{41}\text{Ca}$ ,  $^{43}\text{Ca}(\gamma, p)^{42}\text{K}$ , and  $^{44}\text{Ca}(\gamma, p)^{43}\text{K}$  reactions.

No measured data was found for the  $^{42}\text{Ca}(\gamma, n)^{41}\text{Ca}$ ,  $^{43}\text{Ca}(\gamma, p)^{42}\text{K}$  and  $^{44}\text{Ca}(\gamma, p)^{43}\text{K}$  reactions. The calculated results are plotted in Fig. 2. The calculated  $E_{\text{th}}$  for the  $^{42}\text{Ca}(\gamma, n)^{41}\text{Ca}$ ,  $^{43}\text{Ca}(\gamma, p)^{42}\text{K}$  and  $^{44}\text{Ca}(\gamma, p)^{43}\text{K}$  channels are 11.48, 10.68 and 12.16 MeV, respectively. The distributions of the cross section form peaks around 19.80, 19.40 and 20.60 MeV, respectively. Since these reactions have  $E_{\text{th}}$  around 10 MeV, and the residue nuclei have relatively long half-life, it is necessary to track the decays of  $^{41}\text{Ca}$ ,  $^{42}\text{K}$ , and  $^{43}\text{K}$  after the  $\gamma$

TABLE 1. A summary of the results for the  $\gamma$  induced reactions discussed

Reaction	$^{23}\text{Na}(\gamma, n)^{22}\text{Na}$	$^{25}\text{Mg}(\gamma, p)^{24}\text{Na}$	$^{37}\text{Cl}(\gamma, n)^{36}\text{Cl}$	$^{42}\text{Ca}(\gamma, n)^{41}\text{Ca}$	$^{43}\text{Ca}(\gamma, p)^{42}\text{K}$	$^{44}\text{Ca}(\gamma, p)^{43}\text{K}$
$E_{\text{th}}(\text{MeV})$	12.50	12.06	10.31	11.48	10.68	12.16
Decay mode	$e^+$	$e^-$	$e^-$	EC	$e^-$	$e^-$
Half-life time	2.6027 y	15.00 h	$3.01 \times 10^5$ y	$1.02 \times 10^5$ a	12.32 h	22.30 h
Final residue	$^{22}\text{Na}$	$^{24}\text{Mg}$	$^{36}\text{Ar}$	$^{41}\text{K}$	$^{42}\text{Ca}$	$^{43}\text{Ca}$
<sup>a</sup> Max. of $\sigma$ (mb)	10.58	6.25	37.14	34.47	6.83	4.42
<sup>b</sup> High $\sigma$ range (mb)	19.6–21.2	—	11–23.5	14.2–23	—	—

<sup>a</sup> The maximum value of cross section for the reaction;

<sup>b</sup> The  $E_\gamma$  range where  $\sigma \geq 10$  mb.

therapy.

### C. $^{25}\text{Mg}(\gamma, p)^{24}\text{Na}$

Magnesium is an essential mineral and a cofactor for hundreds of enzymes, it accounts for about 0.05% of the weight of an adult. It is also one of the main components of bone and an essential mineral element in the human body. The normal value of magnesium levels in blood is 0.6–0.95 mmol/L.

The natural abundance of  $^{25}\text{Mg}$  is about 10%. For the  $^{25}\text{Mg}(\gamma, p)^{24}\text{Na}$  reaction,  $^{24}\text{Na}$  is unstable, which allows it to decay to  $^{24}\text{Mg}$  via electron emission with a half-life of 15.00 h. The calculated results are plotted in Fig. 2. The  $E_{\text{th}}$  is 12.06 MeV. The cross sections form a peak around 21 MeV and the largest cross section is 6.25 mb, which is very small compared to the other elements.

The results for the  $\gamma$  induced reactions on isotopes of the human essential elements have been summarized in Table 1. The cross sections for the reactions are very low with the maximum values less than 100 mb. From Table 1, it can be seen that  $^{23}\text{Na}$ ,  $^{37}\text{Cl}$ , and  $^{42}\text{Ca}$  can be activated by  $\gamma$  with  $\sigma > 10$  mb, and the radioactive residue nuclei have a long

half-life. Considering the weight percentages that the elements account for and the importance of them in human body, it is suggested to track the  $^{22}\text{Na}$ ,  $^{42,43}\text{K}$ , and  $^{41}\text{Ca}$  after  $\gamma$  therapy.

## IV. SUMMARY

In this article, the  $\gamma$  induced activated reactions on the stable nuclei of human essential elements have been presented. The possible changes of nuclei are discussed. In  $\gamma$  therapy, the radioactive nucleus produced by the  $\gamma$  induced activated reactions can potentially be one kind of inner radioactivity. The Talys1.4 toolkit was used to predict the cross sections of the reactions. By considering whether the residue nucleus is radioactive and has a long half-life, the  $\gamma$  induced reactions on  $^{23}\text{Na}$ ,  $^{25}\text{Mg}$ ,  $^{37}\text{Cl}$ , and  $^{42,43,44}\text{Ca}$  are investigated, which include the  $(\gamma, n)$  and  $(\gamma, p)$  channels. The cross sections for the reactions are very low with the maximum values less than 100 mb. Taking into consideration the threshold energies, the half-life of the residue nucleus, the percentages of the elements accounting for weight and the importance of them in body, it is suggested to track the  $^{22}\text{Na}$ ,  $^{42,43}\text{K}$ , and  $^{41}\text{Ca}$  after  $\gamma$  therapy.

---

[1] Yuan W J, Ao Y Y, Zhao L, *et al.*  $\gamma$ -ray induced radiolysis of  $[\text{C}_2\text{mim}][\text{NTf}_2]$  and its effects on  $\text{Dy}^{3+}$  extraction. Nucl Sci Tech, 2015, **26**: S10306. DOI: [10.13538/j.1001-8042/hst.26.S10306](https://doi.org/10.13538/j.1001-8042/hst.26.S10306)

[2] Jia W B, Wei Y H, Liu J G, *et al.* Radiolysis of HA in aqueous solutions using gamma rays. Nucl Sci Tech, 2013, **24**: S010308.

[3] El-Beltagi H S, Ahmed O K and El-Desouky W. Effect of low doses gamma-irradiation on oxidative stress and secondary metabolites production of rosemary (*Rosmarinus officinalis* L.) callus culture. Radiat Phys Chem, 2011, **80**: 968–976. DOI: [10.1016/j.radphyschem.2011.05.002](https://doi.org/10.1016/j.radphyschem.2011.05.002)

[4] Wang F, Wang M Y, Liu Y F, *et al.* Obtaining low energy  $\gamma$  dose with CMOS sensors. Nucl Sci Tech, 2014, **25**: 060401. DOI: [10.13538/j.1001-8042/nst.25.060401](https://doi.org/10.13538/j.1001-8042/nst.25.060401)

[5] Masur V M and Mel'nikova L M. Giant dipole resonance in absorption and emission  $\gamma$  rays of by medium and heavy nuclei. Phys Part Nuclei, 2006, **37**: 923–940. DOI: [10.1134/S1063779606060050](https://doi.org/10.1134/S1063779606060050)

[6] Mukul Ish, Roy A, Sugathan P, *et al.* Effect of angular momentum on giant dipole resonance observables in the  $^{28}\text{Si} + ^{116}\text{Cd}$  reaction. Phys Rev C, 2013, **88**: 024312. DOI: [10.1103/PhysRevC.88.024312](https://doi.org/10.1103/PhysRevC.88.024312)

[7] Rodrigues T E, Arruda-Neto J D T, Carvalheiro Z, *et al.* Statistical and direct aspects of  $^{64}\text{Zn}(\gamma, n)$  and  $(\gamma, np)$  decay channels in the giant dipole resonance and quasideuteron energy regions. Phys Rev C, 2003, **68**: 014618. DOI: [10.1103/PhysRevC.68.014618](https://doi.org/10.1103/PhysRevC.68.014618)

[8] Jury J W, Berman B L, Faul D D, *et al.* Photoneutron cross section for  $^{13}\text{C}$ . Phys Rev C, 1979, **19**: 1684–1692. DOI: [10.1103/PhysRevC.19.1684](https://doi.org/10.1103/PhysRevC.19.1684)

[9] Jury J W, Berman B L, Faul D D, *et al.* Photoneutron cross section for  $^{17}\text{O}$ . Phys Rev C, 1980, **21**: 503–511. DOI: [10.1103/PhysRevC.21.503](https://doi.org/10.1103/PhysRevC.21.503)

[10] Woodworth J G, McNeill K G, Jury J W, *et al.* Photonuclear cross section for  $^{18}\text{O}$ . Phys Rev C, 1979, **19**: 1667–1683. DOI: [10.1103/PhysRevC.19.1667](https://doi.org/10.1103/PhysRevC.19.1667)

[11] McNeill K G, Pywell R E, Berman B L, *et al.* Photoneutron cross section for  $^{29}\text{Si}$ . Phys Rev C, 1987, **36**: 1621–1622. DOI: [10.1103/PhysRevC.36.1621](https://doi.org/10.1103/PhysRevC.36.1621)

[12] Koning A J, Hilaire S, Duijvestijn M C, *et al.* User Manual of Talys-1.4. <http://www.talys.eu/download-talys/>

[13] Raynal J. Notes on ECIS94, CEA Saclay Report. No. CEA-N-2772, 1994.

[14] Ma C W, Lü C J, Wei H L, *et al.* An investigation on neutron induced reactions on stable CNO isotopes. Nucl Sci Tech, 2014, **25**: 040501. DOI: [10.13538/j.1001-8042/hst.25.040501](https://doi.org/10.13538/j.1001-8042/hst.25.040501)

[15] Ma C W, Jing R Y, Feng X, *et al.* Investigation of neutron induced reactions on  $^{23}\text{Na}$  by using Talys1.4. Chinese Phys C, 2014, **38**: 104101. DOI: [10.1088/1674-1137/38/10/104101](https://doi.org/10.1088/1674-1137/38/10/104101)

[16] Experimental Nuclear Reaction Data (EXFOR). <https://www-nds.iaea.org/exfor/exfor.htm>

[17] NuDat 2.6. <http://www.nndc.bnl.gov/nudat2>

[18] Micronutrient Information Center. <http://lpi.oregonstate.edu/infocenter/contentnuts.html>

[19] Lin J L and Hsu H Y. Study of sodium ion selective electrodes and differential structures with anodized indium tin oxide. Sensors, 2010, **10**: 1798–1809. DOI: [10.3390/s100301798](https://doi.org/10.3390/s100301798)

[20] Alvarez R A, Berman B L, Lasher D R, *et al.* Photoneutron cross sections for  $^{23}\text{Na}$  and  $^{25}\text{Mg}$ . Phys Rev C, 1971, **4**: 1673–1679. DOI: [10.1103/PhysRevC.4.1673](https://doi.org/10.1103/PhysRevC.4.1673)

[21] Veyssiére A, Beil H, Bergère R, *et al.* A study of the photoneutron contribution to the giant dipole resonance of s-d shell nuclei. Nucl Phys A, 1974, **227**: 513–540. DOI: [10.1016/0375-9474\(74\)90774-X](https://doi.org/10.1016/0375-9474(74)90774-X)